Journal of Environmental Chemical Engineering 10 (2022) 108400

Contents lists available at ScienceDirect

Journal of Environmental Chemical Engineering

journal homepage: www.elsevier.com/locate/jece

On-site regeneration by ultrasound activated persulfate of iron-rich Antipyrine-loaded biochar

Imen Ouiriemmi, Silvia Escudero-Curiel, Marta Pazos *, M. Angeles Sanromán

CINTECX, Universidade de Vigo, Chemical Engineering Department, Campus As Lagoas-Marcosende, 36310 Vigo, Spain

ARTICLE INFO

Editor: Dr. G. Palmisano

Keywords:
Antipyrine
Biochar
On-site regeneration
Advanced oxidation processes
Sulfate radicals

ABSTRACT

Adsorption process has proven its efficiency in the abatement of pharmaceuticals in liquid media, even if large volumes of wastewater need to be treated. Nevertheless, exhausted adsorbent regeneration is economically and environmentally necessary. For this reason, recent studies are aimed at finding new methods of regeneration. In this study, an on-site adsorption-regeneration method was assessed. Initially, a model pharmaceutical, Antipyrine (Apy), has been adsorbed onto a low-cost biochar. Apy adsorption followed a pseudo-second order kinetic and a Langmuir isotherm. In a second step, spent biochar was regenerated by oxidation using $SO_4^{\bullet-}$. To do this, $SO_4^{\bullet-}$ was generated by activation of persulfate by ultrasound and assisted by the iron inherently into the biochar. To facilitate the availability of this iron, the addition of an enhancing agent such as oxalic acid was evaluated. The regenerated biochar proved its stability and reusability achieving an uptake percentage of around 87% after the third adsorption-regeneration cycle. Therefore, this on-site regeneration method could be promising for treating other kinds of adsorbents and resolving the pollution problems caused by the non-controlled throw of the exhausted adsorbents.

1. Introduction

Pharmaceuticals are necessary to control and treat diseases, however, contamination with these products will be of growing concern due to the growing world population, the drugs availability, and the pharmaceuticals persistence [1]. Antipyrine (Apy) is an anti-inflammatory analgesic drug. It is frequently used to treat fever, headache and general pain [2]. This pharmaceutical has relatively weak adsorption in the human body. Therefore, non-negligible amounts of Apy have been discharged in aquatic environments [3]. In fact, Apy and its metabolites were detected in German municipal sewage and surface water in the range of 0.05–0.25 μg/L [4]. Besides, in China, Apy was detected in drinking water plants in the range of 1.34–2.22 ng/L [4]. Thus, the harmful effect of Apy presence in aquatic systems, even at low concentrations, should be taken into consideration [3]. In fact, long-term exposure to Apy leads to mucosae and lungs damage [4]. Although the bad effects of pharmaceuticals on the environment are noticeable even at trace concentrations [5], there is not a regulatory framework for their control until now. Nevertheless, some pharmaceuticals have recently been included in a "Watch List" a list of pollutants prepared by the recent Evolution of the Urban Wastewater Treatment Directive (European Commission), to monitor them and assess their potential dangers and, by consequence, establish an Environmental Quality Standards (EQS) [6].

Many technologies have been integrated to treat wastewater contaminated with pharmaceuticals. However, due to their aromatic structure and their physical characteristics, these pollutants are recalcitrant to biodegradation [7]. Moreover, they have a poor removal efficiency during the conventional treatment processes (coagulation, sediment, and filtration) [8]. In fact, the percentage of Apy removal by these processes is only about 30% [9]. In the last years, sulfate radical based advanced oxidation processes ($SO_4^{\bullet-}$-AOPs) have successfully been used for the oxidation of several pharmaceuticals such as tetracycline [10], sulfadiazine [11], and penicillin [12]. Generally, sulfate radical $SO_4^{\bullet-}$ can be produced by activation of two common precursors: persulfate ($S_2O_8^{2-}$) and peroxymonosulfate (HSO_5^-) [13,14]. These two precursors can be activated by several activators such as heat [14], transition metal ions [15], and ultrasound irradiation [16]. $SO_4^{\bullet-}$-AOPs generate not only $SO_4^{\bullet-}$ but also $HO^{\bullet}$ [15] and they are considered as efficient and eco-friendly processes for the treatment of recalcitrant pollutants [12]. However, they are still not efficient when large volumes of low concentration pollutants need to be treated [17].

* Corresponding author.
E-mail address: mcurras@uvigo.es (M. Pazos).

https://doi.org/10.1016/j.jece.2022.108400
Received 21 December 2021; Received in revised form 29 July 2022; Accepted 4 August 2022
Available online 5 August 2022

At industrial scale, adsorption seems to be among the most appropriate technologies for wastewater treatment. Adsorption facilitates the quick remediation of large volumes of wastewater with simple and relatively inexpensive equipment [18,19]. In the concept of circular economy, the use of adsorbents derived from modified waste materials has recently interested many researchers [20]. Among these adsorbents, biochar is a carbonaceous material manufactured from several biomass feed stocks. Eco-friendly nature, low cost, and removal efficiency are among the advantages of this adsorbent [21]. Despite the advantages of adsorption treatment, the uncontrolled disposal of exhausted adsorbent without any post-treatment is another environmental issue. Many studies have addressed the regeneration of these exhausted adsorbents by means of different techniques. Among them, $SO_4^{\bullet-}$-AOPs seem to be efficient as for example the regeneration rate of fluoxetine loaded biochar by a ferrous-peroxymonosulfate treatment was around 81% [6].

To the best of our knowledge, the on-site regeneration of carbonaceous adsorbent by using $SO_4^{\bullet-}$-AOPs is still scarce and this is the first approach in which ultrasound is coupled to the regeneration process by $SO_4^{\bullet-}$. Therefore, in this study, an on-site adsorption-regeneration process has been developed for the abatement of Apy, a pharmaceuticals model, in wastewater. The first step consists of the adsorption of this pharmaceutical onto biochar which is a low-cost adsorbent. Then, the second step consists of the regeneration of the exhausted biochar by the $SO_4^{\bullet-}$ oxidation of Apy on the adsorbent. Persulfate (PS) was used as $SO_4^{\bullet-}$ precursor and both ultrasound (US) and iron were evaluated as activators.

2. Materials and methods

2.1. Materials

Antipyrine (Apy) with purity higher 99% supplied by Sigma-Aldrich was evaluated as a model pollutant and solutions were prepared by using Milli-Q grade water as solvent. Biochar, used as adsorbent in this study, was provided by Ibero Massa Florestal S. A. (UI, Oliveira de Azeméis, Portugal). It was crushed (d≤500 μm) by a Retsch cutting mill SM100 then thermally pre-treated as described in a previous study [1].

All used reagents have been depicted in Supplementary Material (Table SMT1).

2.2. Experimental set-up

2.2.1. Adsorbent characterization

Scanning electron microscope (SEM) images have been applied to evaluate the biochar surface morphology. The metal content was measured by inductively coupled plasma mass spectrometry (ICP-MS). For doing this analysis, samples were previously digested according to the Danish Standard DS259. Fourier transform infrared (FTIR) spectroscopy has been applied to have an idea about the biochar surface functional groups. Specific surface area, pore size, and pore volume have been determined by N_2 adsorption-desorption isotherm applying Brunauer-Emmett-Teller (BET) method using a Micromeritics ASAP2020. All the above analyzes have been conducted at the scientific-technological support center for research (Centro de Apoio Científico-Tecnolóxico á Investigación) C.A.C.T.I., University of Vigo, (Vigo, Spain).

2.2.2. Adsorption

Adsorption experiments were conducted in graduated centrifuge tubes (max capacity 50 mL). Firstly, 1 g of biochar was mixed with 50 mL of Apy solution with a known initial concentration (C_0) that was varied from 30 to 100 mg L^{-1}. The pH of the medium was not modified, being around 7.5 during all the experiments. The tubes were shaken in a rotary tube shaker (JP Selecta 7001723 Movil-Rod) at 25 °C. Secondly, the biochar was separated from the solution by centrifugation (Hettich Centrifuge Rotina 380 R) at 8000 rpm during 15 min. All experiments were performed in duplicate. Apy concentration before, during and after adsorption was measured in the supernatant by High- Performance Liquid Chromatography (HPLC) Agilent 1260 equipped with a column Zorbax Eclipse XDB-C-8 4.6 × 150 mm 5-micron (Agilent Technologies) and coupled with a DAD detector (Agilent) selected at optimum wavelengths of 242 nm. A 90:10 (v/v) water/acetonitrile mixture at 1 mL min^{-1} flow rate was used as mobile phase.

The Apy uptake and the maximum Apy removal percentage were calculated according to the expressions depicted in Table SMT2. After that, three kinetic models (pseudo-first order (PFO), pseudo-second order (PSO), and intra-particle diffusion (IPD)), as well as three isotherm models (Langmuir, Freundlich and Temkin) were used to fit the experimental data. The expressions and parameters of all these models are detailed in Table SMT3.

2.2.3. Desorption

Desorption assays were conducted in graduated centrifuge tubes using the same ratio adsorbent/liquid and used in the adsorption experiments (Section 2.2.2.). Three different eluents were tested to desorb Apy from biochar; E_1: acetonitrile, E_2: acetonitrile/water (50/50), and E_3: acetonitrile/water (80/20) with NH_4Cl (0.2 M) [19]. The eluent that gave best desorption results was used to quantify the amount of Apy on the adsorbent before and after the regeneration step. More details about the desorption process can be found in Supplementary Materials section 1.2.2. and Table SMT4.

2.2.4. Apy degradation in aqueous media

Several degradation processes were performed in liquid media: PS; US/PS: US in the presence of PS; PS/Fe(II): PS in the presence of iron; and US/PS/Fe(II): US in the presence of both PS and iron. More details about the experimental conditions can be found in Table 1. It is important to be mentioned that, for PS/Fe(II) and US/PS/Fe(II), the pH of the medium is acid during the experiments because of the acidic effect of sodium persulfate.

2.2.5. Biochar regeneration

Several tests were conducted to regenerate exhausted biochar obtained by mixing 1 g of adsorbent with 50 mL of 30 mg L^{-1} of Apy solution. After the adsorption step, the graduated centrifuge tubes were centrifuged (Hettich Zentrifugen D-78532 Tuttlingen Rotina 380 R, Germany) at 8000 rpm for 15 min. Then, the supernatant was replaced by 50 mL of the oxidation solution determined in the preliminary assays. Finally, the mixture was sonicated in an ultrasonic bath (DU-65 digital ultrasonic cleaner), operating at a fixed frequency of 40 KHz at 50% power at 20 °C. pH was monitored to be acid during the experiments. More details about the biochar regeneration experiments can be found in Supplementary Materials section 1.2.4.

2.2.6. Adsorbent reusability

The reusability of the biochar was evaluated in three adsorption-regeneration cycles. In each cycle, 50 mL of 30 mg L^{-1} of Apy solution was mixed with 1 g of regenerated adsorbent for 2 h.

3. Results and discussion

3.1. Apy adsorption on biochar

3.1.1. Contact time and initial Apy concentration effects on the adsorption

To determine the effect of contact time and Apy initial concentration, the temporal evolution of the adsorption profile was studied at five different Apy initial concentrations (Fig. 1a) during 1 h. The adsorption profiles showed an increase of Apy adsorption efficiency along with contact time as well as a quick Apy uptake in the first 5 min. This fact might be attributed to the availability of uncovered surfaces and many empty active sites at the beginning of the adsorption process [22]. After

Table 1
Experimental conditions of the processes used for Apy degradation in liquid media during 1 h.

Method		Apy concentration (mg L^{-1})	PS concentration (mM)	Fe^{2+}concentration (mM)	Frequency (kHz)	Power (%)
First set of experiments	US	10	–	–	40	50
	PS 100 mM	10	100	–	–	–
	US/PS 100 mM	10	100	–	40	50
	US/PS 100 mM/Fe(II) 0.1 mM	10	100	0.1	40	50
	US/PS 100 mM/Fe(II) 0.3 mM	10	100	0.3	40	50
Second set of experiments	US/PS 30 mM/Fe(II) 0.1 mM	10	30	0.1	40	50
		30	30	0.1	40	50
	US/PS 50 mM/Fe(II) 0.1 mM	10	50	0.1	40	50
		30	50	0.1	40	50
	US/PS 100 mM/Fe(II) 0.1 mM	10	100	0.1	40	50
		30	100	0.1	40	50
	US/PS 100 mM/Fe(II) 0.3 mM	10	100	0.3	40	50

these initial stages, as time goes on, the active sites become more occupied by the pollutant and the adsorption rate diminishes [23]. This could explain the slowing of Apy adsorption after the first few minutes until reaching equilibrium. The evaluation of the Apy initial concentration effect on the adsorption permits to note that the removal efficiency decreased from 97.7% to 68.4% when the Apy initial concentration rose up from 30 to 100 mg L^{-1}. This result can be attributed to the fact that at lower Apy initial concentration the ratio of the biochar active sites to the total Apy is high and, as consequence, all Apy molecules can interact with the biochar and be uptaken from the solution [22,24]. Besides, it can be noticed that the increase of the Apy initial concentration led to an increase of the uptake which achieved an equilibrium value around 3.44 mg g^{-1}. This result can be explained by the increase of the Apy molecules in the solution meaning the increase of the concentration gradient. Consequently, the arrival of the Apy molecules to the biochar surface became easier which led to a higher occupation of biochar active sites [22,25]. From Fig. 1a, it can be also concluded that for an initial Apy concentration higher than 90 mg L^{-1} (100 mg L^{-1}), no significant increase in the pharmaceutical uptake was observed. Consequently, the material got saturated when using an initial concentration of 90 mg L^{-1}.

3.1.2. Apy adsorption kinetics

PFO and PSO have been used to fit the kinetic experimental data and the obtained results are summarized in Table SMT6. From this table, it can be concluded that PSO model was more suitable than PFO model in characterizing the adsorption process. In fact, PSO showed higher correlation coefficients, lower standard error of estimate (SEE), and better concordance between the experimental adsorption uptakes and those mathematically calculated using the kinetic model equations. These results suggest that chemisorption is one of the mechanisms implicated in the adsorption process [26]. The suitability of PSO to fit the experimental adsorption kinetic data of other pharmaceuticals (diclofenac and cephalexin) on biochar has been previously reported [27]. To have a better idea about the adsorption mechanism, BET isotherms were applied to obtain the characterization of the surface area and pore distribution and have been represented in SMF1. Biochar specific surface area, pore size, and pore volume are 270 m^2 g^{-11}, 20.06 Å, and 0.136 cm^3 g^{-1} respectively. According to the IUPAC classification [28], N_2 adsorption-desorption isotherm represented in Fig. SMF1. is type II. This suggests a dominant macroporous structure of biochar, and the adsorption takes place in multiple layers. Furthermore, the IPD model was applied to the kinetic experimental data and the obtained results have been summarized in Table SM7. The representation of q versus $t^{0.5}$ presented in Fig. 1b did not satisfy a linear relationship. Consequently, IPD is not the only controlling step of the Apy adsorption onto biochar and two or more steps were implicated [29]. The poor adjustment of one stage IPD fit to the experimental data is given by the low R^2 values ($0.706 \leq R^2 \leq 0.885$) and the high SEE values ($0.02 \leq SEE \leq 0.126$) (Table SMT7). However, Fig. 1b shows that q versus $t^{0.5}$ curve can be divided into three linear zones; zone I: $0.67 \leq t^{0.5} \leq 2.17$; Zone II: $2.17 \leq t^{0.5} \leq 5.46$; and zone III: $5.46 \leq t^{0.5} \leq 7.74$. Much better results have been obtained by using three stages IPD fit ($0.905 \leq R^2 \leq 0.999$ and $0.001 \leq SEE \leq 0.045$) (see Table SMT7) by comparison to those obtained by one stage IPD fit. Quesada and coworkers attributed zone I to film diffusion step, zone II to IPD step, and zone III to the equilibrium of the adsorption system [30]. These three steps have also been identified by Valusamy and coworkers during the adsorption of another pharmaceutical pollutant, ciprofloxacin, onto biochar derived from soap nut seeds [21].

3.1.3. Adsorption isotherms

Isotherms experiments have been conducted at 25 °C for 2 h and the obtained results are shown in Fig. 1c. Three isotherm models have been applied to the experimental data and the calculated parameters of these models are summarized in Table SMT8. Langmuir model gave the best fit as higher correlation coefficient and lower SEE were obtained using this model. Moreover, experimental maximum uptake and that calculated using this model are almost the same (3.53 and 3.49 mg g^{-1}, respectively). Accordingly, a homogeneous distribution of active sites on the biochar surface and a monolayer coverage of Apy onto this adsorbent has been suggested. Similar results have been obtained during the adsorption of diclofenac and cephalexin on activated biochar [27]. This uptake (3.53 mg g^{-1}) is lower than that found by Puga and coworkers [31] after 24 h of Apy adsorption onto three monolithic carbonaceous aerogels; NQ30A (32 mg g^{-1}), NQ60A (49.7 mg g^{-1}), and NQ80A (20 mg g^{-1}). However, biochar is still attractive taking into account its quick adsorption, low price, and environmentally friendly application.

3.2. Regeneration studies

3.2.1. Apy degradation in aqueous media

Before evaluating the Apy on-site regeneration, several treatments were performed in aqueous media to know their effect on the degradation of this pollutant. From Fig. 2a, different responses of the pharmaceutical to the treatment processes can be observed. Although US has been reported to be more effective than single PS oxidation for the majority of organic compounds [32], this treatment seems to be unable to degrade Apy even at a low concentration (10 mg L^{-1}). Better results have been obtained using PS, as almost 27% of the Apy initially existing was oxidized after 1 h treatment. A better performance of single PS by comparison with US was also reported in some previous studies [33,34]. Yang and coworkers [32] justified this result by the presence of special molecular structures. After that, the synergistic effects of US and PS have

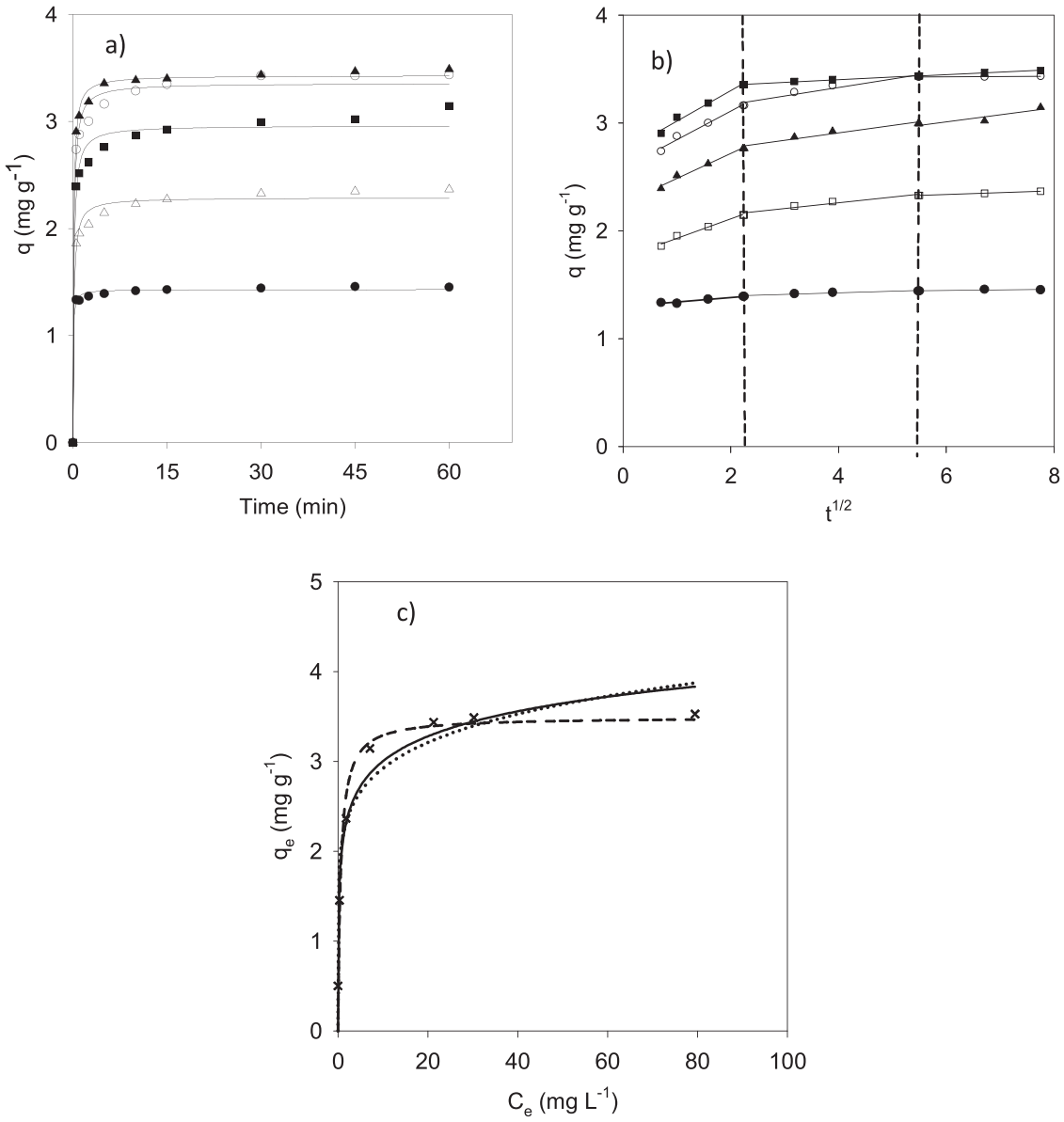

Fig. 1. Apy adsorption on biochar: (a) uptake profile during 1 h: initial Apy concentrations: (•) [Apy]= 30 mg L^{-1}; (Δ) [Apy]= 50 mg L^{-1}; (■) [Apy]= 70 mg L^{-1}; (○) [Apy]= 90 mg L^{-1}; (▲) [Apy]= 100 mg L^{-1}; lines represent PSO kinetic adjustment. (b) intra-particle diffusion plot at different initial Apy concentrations: (•) [Apy]= 30 mg L^{-1}; (□) [Apy]= 50 mg L^{-1}; (▲) [Apy]= 70 mg L^{-1}; (○) [Apy]= 90 mg L^{-1}; (■) [Apy]= 100 mg $L^{-1}$and (c) Isotherm study: (×) experimental data obtained after 2 h of contact time fitted by: (- - -) Langmuir adjustment; (.) Freundlich adjustment; and (▬) Temkin adjustment. Experimental conditions: $m_{adsorbent}$= 1 g; V= 50 mL; T = 25 °C.

been studied by using US/PS process. Yang et al. [32] confirmed the role of US in the homolysis of the O-O bond in PS by cavitation and high temperatures and pressures attained in the solution to produce $SO_4^{\bullet-}$ according to Eq. 1. Moreover, they stated that the violent turbulence caused by US increases the mass transfer in the solution. This might explain the increase of Apy degradation percentage to reach almost 34%. To further increase the Apy degradation, iron ions were added to US/PS system to double-activate PS according to Eq. 2 [35]. Thus, two iron concentrations (0.1 and 0.3 mM) were tested under the same experimental conditions (Table 1). The results, depicted in Fig. 2a, showed a big enhancement of the process performance. Total pollutant degradation was obtained with both iron concentrations after 1 h of treatment. These results illustrated that PS can be highly activated by Fe^{2+} and US. Consequently, US/PS/Fe(II) was the most appropriate process for Apy degradation.

$$S_2O_8^{2-} + US \rightarrow 2\ SO_4^{\bullet-} \quad (1)$$

$$S_2O_8^{2-} + Fe^{2+} \rightarrow SO_4^{\bullet-} + SO_4^{2-} + Fe^{3+} (k = 27 Ms^{-1}) \quad (2)$$

A second set of experiments was carried out to test the influence of initial concentrations of Apy, PS and Fe^{2+} on the US/PS/Fe(II) process performance. The obtained results (Fig. 2b) showed that, in the same experimental conditions, the degradation percentage decreased as the initial [Apy] increased from 10 to 30 mg L^{-1}. This may be explained by the fact that with an elevated initial [Apy], a competition between the residual Apy and its related intermediates for the produced oxidants ($HO^{\bullet}$ and $SO_4^{\bullet-}$) could take place [36]. In addition, it can be seen that, for the same initial [Fe^{2+}], 0.1 mM, the increase of the initial [PS] from 30 to 100 mM induced the enhancement of Apy degradation percentage. Actually, the percentage increased from 68.8% to 100% for Apy initial concentration of 10 mg L^{-1} while it rose up from 11.6% to 77.8% for Apy initial concentration of 30 mg L^{-1}. This is explained by the fact that higher initial [PS] induces higher $SO_4^{\bullet-}$ production, which translates into

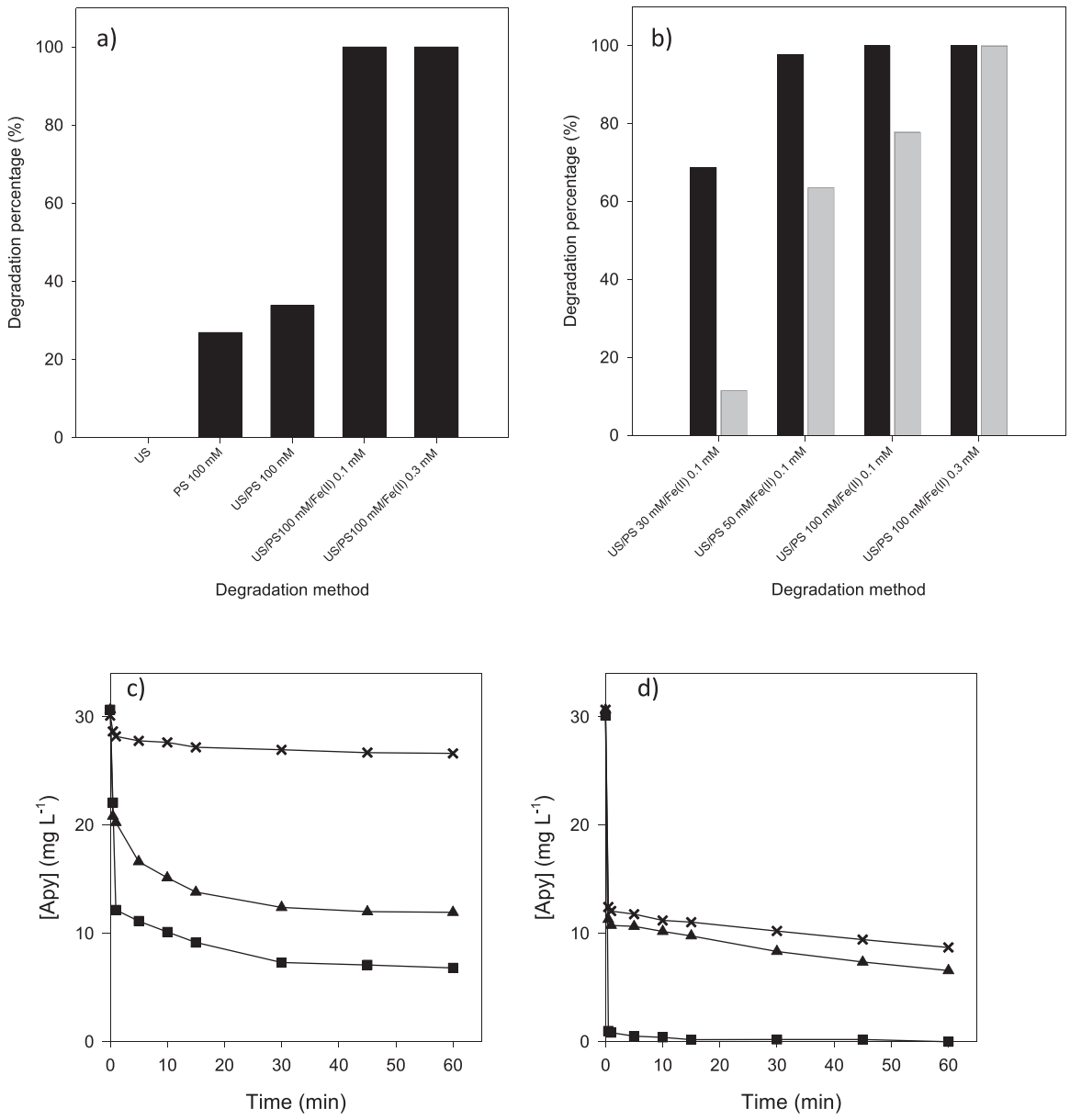

Fig. 2. Apy degradation in aqueous solution under different treatments: (a) Apy 10 mg L^{-1}; (b) Apy 10 mg L^{-1} (black bars) and 30 mg L^{-1} (Gray bars) and profiles of degradation in aqueous media of Apy 30 mg L^{-1} during 1 h of treatment by (c) US/PS/Fe(II) process [Fe^{2+}]= 0.1 mM and (d) US/PS/Fe(II) process [Fe^{2+}]= 0.3 mM; (×) [PS]= 30 mM; (▲) [PS]= 50 mM; and (■) [PS]= 100 mM. Experimental conditions: $V_{solution}$= 50 mL; T = 20 °C; treatment time= 1 h.

better Apy degradation results. Similar results have been previously reported by Zhou et al. [36]. For Apy initial concentration of 30 mg L^{-1}, total degradation was not obtained with Fe^{2+} 0.1 mM even when 100 mM of PS was used. So, the $SO_4^{\bullet-}$ produced seemed not to be enough to degrade all the Apy molecules. Therefore, initial [Fe^{2+}] was increased from 0.1 to 0.3 mM, while initial [PS] was fixed at 100 mM. By increasing the Fe^{2+} concentration from 0.1 to 0.3 mM, total Apy degradation was achieved for the two Apy initial concentrations tested. Thus, higher amounts of Fe^{2+} improved $SO_4^{\bullet-}$ production (Eq. 2) increased the Apy decomposition. Similar results were found by Rao et al. [37] during the degradation of carbamazepine by Fe(II)-activated PS.

To better understand the effect of [PS] and [Fe^{2+}] on the Apy degradation, the oxidation of 50 mL of this pharmaceutical solution 30 mg L^{-1} was monitored for 1 h (Fig. 2c and d). For that, US/PS/Fe(II) degradation experiments were carried out by varying [PS] ([PS]= 30;50;100 mM) and [Fe^{2+}] ([Fe^{2+}]=0.1;0.3 mM). The results depicted in Fig. 2c and d demonstrated that, for all experiments, Apy degradation is characterized by a two-stage kinetic; a very quick decay within the very first 30 s followed by a much slower one. The $SO_4^{\bullet-}$ production rates, calculated according to Eq. 2, have been summarized in Table SMT9. From these data, it can be concluded that, when increasing $S_2O_8^{2-}$ and/or Fe^{2+} initial concentrations, a faster reaction between these reagents takes place which led to a quicker $SO_4^{\bullet-}$ production and then faster Apy oxidation. After 30 s, Apy degradation slowed down. This may be due to the competition between Apy and its by-products, produced during the reaction time, for the available $SO_4^{\bullet-}$. Similar results have been previously reported by Rao et al. [37] when degrading carbamazepine by Fe(II)-activated PS.

3.2.2. *Desorption studies*

Several eluents were tested to desorb Apy from the biochar to quantify the persistent Apy on the adsorbent after the regeneration step, and then determine the regeneration treatment efficiency. For this

purpose, 1 g of the exhausted biochar was mixed with 50 mL of the selected eluent. Table SMT10 summarizes the obtained results. According to this table, high desorption efficiencies (>87%) were obtained using the three eluents. Increasing the treatment time from 2 to 16 h did not have a notable effect on desorption efficiency. Therefore, from a practical and economical point of view, the contact time was fixed at 2 h. As E_3 gave the best results, two successive desorptions with this eluent (V=0.05 L) have been done during 1 h each in the aim of obtaining better desorption results (for more details see Supplementary Materials section 1.2.2. The use of this latter desorption method gave total desorption of Apy from the exhausted biochar. Therefore, this method was used to quantify the persistence of Apy on the biochar after the regeneration in solid matrix experiments.

3.2.3. Adsorbent regeneration

The results presented in Fig. 3a showed that the adsorbent regeneration by US was around 2.7%. As US was not able to degrade Apy (Fig. 3a), this regeneration percentage could be caused by the Apy desorption from biochar surface due to the US treatment [38]. This result has been confirmed by measuring Apy concentration in liquid fraction after 1 h of biochar regeneration by US (No Apy has been detected in liquid fraction for the rest of experiments). The feasibility of using US to desorb pharmaceuticals from adsorbents in aqueous media has been already proven by Zhang and coworkers [39] during the desorption of chloramphenicol from powdered activated carbon. The PS concentration (100 mM) that gave the best Apy degradation in the liquid media tests (see Section 3.2.1) was applied to regenerate the exhausted adsorbent. As expected, when using this PS concentration, high regeneration percentage (around 70%) was obtained. To further enhance the biochar regeneration, PS was activated using iron and/or US. US/PS 100 mM system gave better results than PS alone, achieving up to 79.2% of biochar regeneration. This good result may be explained by the

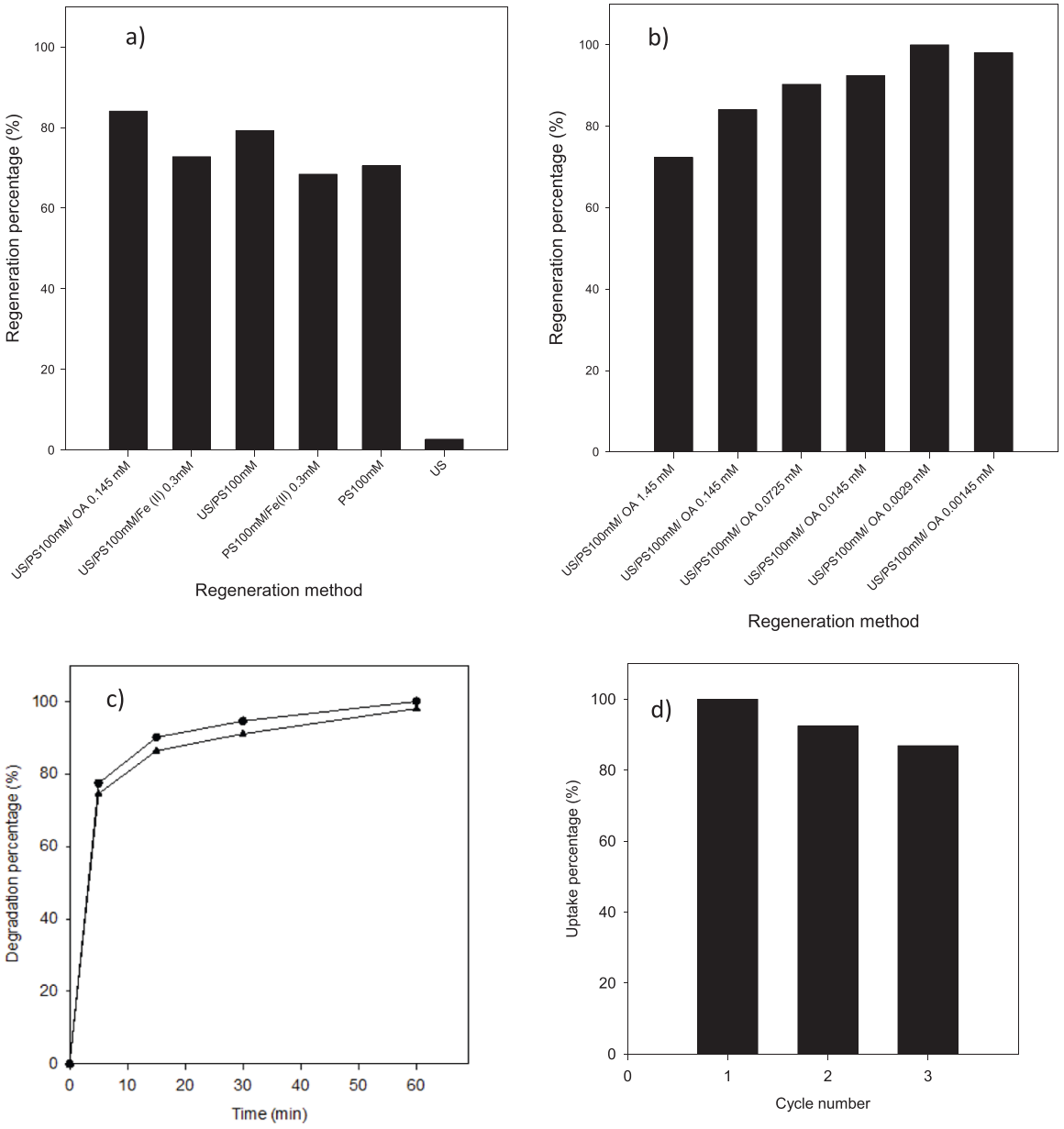

Fig. 3. Biochar regeneration(Experimental conditions: $m_{exhausted\ adsorbent}$= 1 g; $V_{solution}$= 50 mL; T = 20 °C; treatment time=1 h): (a) preliminary evaluation under different regeneration processes; (b) effect of the OA concentration; (c) Apy profile during treatment under US/PS100 mM/OA process operating with (•) [OA]= 0.0029 mM and (▲)[OA]= 0.00145 mM; and (d) Apy uptake onto biochar during three adsorption-regeneration cycles carried out after 2 h with $m_{adsorbent}$= 1 g; $V_{solution}$= 50 mL and T = 25 °C.

synergistic effect of PS decomposition (according to Eq. 1) and the Apy desorption by US (previously mentioned). By adding iron, low regeneration percentages have been obtained. Actually, the regeneration percentage of PS100 mM/Fe(II) 0.3 mM system decreased by around 1.6% by comparison to PS 100 mM system and that of US/PS 100 mM/Fe(II) 0.3 mM system decreased by almost 6.5% by comparison to US/PS 100 mM system. To explain this decrease in the regeneration performance, the mineral content of the biochar was evaluated, and the obtained results are shown in Table SMT11. From this table, it can be noticed that biochar contains several metals such as Ni, Zn, Mn, and especially Fe (14,536.54 g per Kg of biochar). These metals can act as PS activators, therefore adding external iron can have a negative effect on the biochar regeneration as the excess of the activator agent could have a scavenger effect for the produced sulfate radicals according to Eq. 3 as Escudero-Curiel and coworkers [6] pointed out. Accordingly, to improve the regeneration process, it was suggested the use of a chelating agent, a substance that makes iron more available for PS activation. Xue and coworkers [40] found that oxalic acid is a great and environmentally friendly iron-chelating agent. In fact, the best heterogeneous oxidation of PCP in the magnetite/H_2O_2 system was obtained when using this acid as a chelating agent, by comparison to five other chelating agents (ethylene diamine, tetraacetic acid, citrate, succinate, tartrate…). Therefore, oxalic acid (OA) was selected as iron-chelating agent. As expected, US/PS 100 mM/ OA 0.145 mM system gave better results and the regeneration percentage achieved 84%. This result is encouraging; this is why further tests were carried out to optimize OA concentration. As shown in Fig. 3b, by decreasing OA concentration from 1.45 mM to 0.0029 mM, the regeneration percentage increased from 72.4% to 100%. The bad effect of higher concentrations of OA can be explained by the reaction of this latter with $SO_4^{\bullet-}$ and $HO^{\bullet}$ [6] which badly affect the regeneration performance. At an OA concentration two times less than 0.0029 mM, almost 98% was regenerated. In order to finally select the best of the two OA concentrations tested, it was necessary to monitor the biochar regeneration during the treatment time. The biochar regeneration profiles when using these two concentrations (Fig. 3c) seemed to be quite similar; a quick regeneration during the first five minutes followed by a slower regeneration during the rest of the treatment time. Therefore, from an economical point of view, 0.00145 mM is the most suitable OA concentration to work with.

$$Fe^{2+} + SO_4^{\bullet-} \rightarrow \quad Fe^{3+} + SO_4^{2-} \tag{3}$$

3.3. Adsorbent reusability

Under the best regeneration conditions previously found, biochar was successfully regenerated and three consecutive adsorption-regeneration cycles were conducted. As it is clear in Fig. 3d, the Apy uptake percentages after the second and the third cycle were comparable to that after the first cycle. This result suggests that almost all the Apy adsorbed on the biochar surface was oxidized and the sites were again available to interact with other molecules. Moreover, this result suggests that biochar was still stable after the oxidation step. To confirm this, FTIR and SEM analyses have been done. FTIR spectra during the three adsorption-regeneration cycles are shown in Fig. SMF2 and SMF3. In SMF1, it can be observed the changes in the pristine biochar after Apy adsorption. Apy, with two aromatic rings, contributes to increase the band at 3027 cm^{-1} where appear the modes of tension vibration of C-H bonds of aromatic groups and the bending of these groups at 874–750 cm^{-1}. In SMF3 an intensification in the same bands is detected after each adsorption process and a decrease in the same bands after each regeneration process. SMF3 showed similar spectra among the pristine, adsorbed, and regenerated biochar. Each spectrum showed the presence of peaks in the range of 3000–2850 cm^{-1} which correspond to aliphatic C-H stretching vibration [41]. The most obvious peak at around 3443 cm^{-1} was attributed to the O-H group [42]. The peak around 1562 cm^{-1} refers to C═C stretching vibration in conjugated olefin while that around 1692 cm^{-1} was attributed to the carbonyl functionality [43]. The presence of cellulose and hemicelluloses was demonstrated by the C-O-C symmetric stretching at 1118 cm^{-1} [44]. Other elongation vibrations from 1400 to 1000 cm^{-1} were attributed to the C-O and C-H bonds, which indicated the presence of ester and alcohol groups [6]. FTIR analyses prove the stability of the adsorbent as it still has the same morphology during treatment time. The biochar stability is also confirmed by the SEM images shown in Fig. SMF4. In fact, the biochar surface kept the same morphology during all the adsorption-regeneration cycles; it was rough and contained pores, cracks, and fissures. During each cycle, three separation solution-biochar techniques (centrifugations) were necessary which increases the probability of losing the biochar powder. This may be the cause of the small decrease in the uptake percentage from 100% in the first cycle to 92% and 87%, respectively, in the second and the third cycle. Using the biochar as an adsorbent more than one time is an encouraging result from an economic and environmental point of view.

4. Conclusions

In this study, on-site regeneration with $SO_4^{\bullet-}$ of a cheap and environmentally friendly carbonaceous adsorbent, biochar, was evaluated for the management of exhausted adsorbents obtained by the treatment of effluents polluted with Apy. In a first step, the selected biochar, demonstrated to be an appropriate material for the Apy removal. PSO and Langmuir isotherm described well the adsorption process and a monolayer coverage of Apy onto this adsorbent has been suggested. After that, the regeneration of the biochar by using sulfate radicals was accomplished. A new approach of activation combining US and biochar metal self-containing was carried out. Thus, exhausted biochar was regenerated by means of a combined system of US/PS 100 mM. In this system, sulfate radicals were produced by the decomposition of PS in the presence of US and metal self-containing as activators. Therefore, it was not necessary to add extra iron or metal to activate PS as biochar was a mineral-rich material. Furthermore, the addition of OA as a chelating agent enhanced the regeneration process until achieving complete removal of the pollutant because it made metals more available for PS activation. Finally, biochar stability and reusability have been proved by FTIR and SEM analyses as this adsorbent maintained its morphology and performance during three adsorption-regeneration cycles. Using more than one time the biochar as an adsorbent is an encouraging result from an economic and environmental point of view. Therefore, the sulfate radical oxidation method is worthy to be tested for the regeneration of other kinds of adsorbents.

CRediT authorship contribution statement

Marta Pazos and Angeles Sanróman: Conceptualization. **Imen Ouiriemmi and Silvia Escudero-Curiel**: Investigation. **Marta Pazos and Angeles Sanróman**: Resources. **Imen Ouiriemmi**: Data curation. **Imen Ouiriemmi**: Writing – original draft. **Marta Pazos, Angeles Sanróman and Silvia Escudero-Curiel**: Writing – review & editing. **Marta Pazos and Angeles Sanróman**: Funding acquisition. All authors have read and agreed to the published version of the manuscript.

Declaration of Competing Interest

The authors declare that they have no known competing financial interests or personal relationships that could have appeared to influence the work reported in this paper.

Data availability

Data will be made available on request.

Acknowledgements

This research has been financially supported Project PID2020-113667GB-I00 funded by MCIN/AEI/10.13039/501100011033 and PDC2021-121394-I00 funded by MCIN/AEI/10.13039/501100011033 and by the European Union Next GenerationEU/PRTR, Xunta de Galicia and European Regional Development Fund (ED431C 2021-43). Silvia Escudero-Curiel thanks Universidade de Vigo for her fellowship.

Appendix A. Supporting information

Supplementary data associated with this article can be found in the online version at doi:10.1016/j.jece.2022.108400.

References

[1] L. Mayerhuber, S. Trattner, S. Luger, G. Weigelhofer, C. Hametner, P. Fruhmann, J. Electroanal. Chem. 886 (2021), 115110.
[2] M.Q. Cai, L. Feng, J. Jiang, F. Qi, L.Q. Zhang, Water Res. 47 (2013) 2830–2842.
[3] X.H. Jia, L. Feng, Y.Z. Liu, L.Q. Zhang, Chem. Eng. J. 309 (2017) 646–654.
[4] M. Cai, L. Zhang, F. Qi, L. Feng, J. Environ. Sci. 25 (2013) 77–84.
[5] M. Chauhan, V.K. Saini, S. Suthar, J. Porous Mater. 27 (2020) 383–393.
[6] S. Escudero-Curiel, U. Penelas, M.Á. Sanromán, M. Pazos, Chemosphere 268 (2021), 129318.
[7] K. Dadididou, J.M. Monteagudo, E. Chatzisymeon, A. Durán, A.J. Expósito, Sep. Purif. Technol. 172 (2017) 227–235.
[8] P. Liu, X. Wang, J. Lu, Y. Li, B. Hou, L. Feng, Environ. Sci. Pollut. Res. 27 (2020) 40837–40847.
[9] T. Deblonde, C. Cossu-Leguille, P. Hartemann, Int. J. Hyg. Environ. Health 214 (2011) 442–448.
[10] F. Shao, Y. Wang, Y. Mao, T. Shao, J. Shang, Chemosphere 261 (2020), 127844.
[11] T. Liu, K. Wu, M. Wang, C. Jing, Y. Chen, S. Yang, P. Jin, Chemosphere 262 (2021), 127845.
[12] Y. Zhang, B.T. Zhang, Y. Teng, J. Zhao, L. Kuang, X. Sun, Sep. Purif. Technol. 254 (2021), 117617.
[13] T. Zhou, X. Zou, J. Mao, X. Wu, Appl. Catal. B 185 (2016) 31–41.
[14] C. Tan, N. Gao, Y. Deng, N. An, J. Deng, Chem. Eng. J. 203 (2012) 294–300.
[15] H. Liu, T.A. Bruton, W. Li, J.V. Buren, C. Prasse, F.M. Doyle, D.L. Sedlak, Environ. Sci. Technol. 50 (2016) 890–898.
[16] W.P. Fagan, J. Zhao, F.A. Villamena, J.L. Zweier, L.K. Weavers, Ultrason. Sonochem. 67 (2020), 105172.
[17] S.O. Ganiyu, E.D. van Hullebusch, M. Cretin, G. Esposito, M.A. Oturan, Sep. Purif. Technol. 156 (2015) 891–914.
[18] J.A. Gonzalez, M.E. Villanueva, L.L. Piehl, G.J. Copello, Chem. Eng. J. 280 (2015) 41–48.
[19] A.M. Diez, M.A. Sanroman, M. Pazos, Catal. Today 313 (2018) 122–127.
[20] S. Escudero-Curiel, V. Acevedo-García, M.Á. Sanromán, M. Pazos, Electrochim. Acta (2021), 138694.
[21] K. Velusamy, S. Periyasamy, P.S. Kumar, T. Jayaraj, R. Krishnasamy, J. Sindhu, D. Sneka, B. Subhashini, D.-V.N. Vo, Environ. Pollut. 287 (2021), 117632.
[22] B. Hayoun, M. Bourouina, M. Pazos, M.A. Sanroman, S. Bourouina-Bacha, Appl. Sci. 10 (2020) 3271.
[23] R.K. Gautam, V. Rawat, S. Banerjee, M.A. Sanromán, S. Soni, S.K. Singh, M. C. Chattopadhyaya, J. Mol. Liq. 212 (2015) 227–236.
[24] H.R. Pouretedal, N. Sadegh, J. Water Process. Eng. 1 (2014) 64–73.
[25] G.B. Oguntimein, Adv. Res. Text. Eng. 1 (2016) 1008–1014.
[26] Y. Ho, J. Hazard. Mater. 136 (2006) 681–689.
[27] Z. Shirani, H. Song, A. Bhatnagar, Sci. Total Environ. 745 (2020), 140789.
[28] K.S.W. Sing, Pure Appl. Chem. 64 (1982) 2201–2218.
[29] R. Elmoubarki, F.Z. Mahjoubi, H. Tounsadi, J. Moustadraf, M. Abdennouri, A. Zouhri, A. El Albani, N. Barka, Water Resour. Ind. 9 (2015) 16–29.
[30] H.B. Quesada, L.F. Cusioli, C.O. Bezerra, A.T. Baptista, L. Nishi, R.G. Gomes, R. Bergamasco, J. Chem. Technol. Biotechnol. 94 (2019) 3147–3157.
[31] A. Puga, E. Rosales, M. Sanromán, A.M. Pazos, Chemosphere 248 (2020), 125995.
[32] L. Yang, J. Xue, L. He, L. Wu, Y. Ma, H. Chen, H. Li, P. Peng, Z. Zhang, Chem. Eng. J. 378 (2019), 122146.
[33] S. Nasseri, A.H. Mahvi, M. Seyedsalehi, K. Yaghmaeian, R. Nabizadeh, M. Alimohammadi, G.H. Safari, J. Mol. Liq. 241 (2017) 704–714.
[34] R.L. Yin, W.Q. Guo, H.Z. Wang, J.S. Du, X.J. Zhou, Q.L. Wu, H.S. Zheng, J.S. Chang, N.Q. Ren, Chem. Eng. J. 335 (2018) 145–153.
[35] C. Cai, L. Wang, H. Gao, L. Hou, H. Zhang, J. Environ. Sci. 26 (2014) 1267–1273.
[36] X. Zhou, T. Zhou, J. Mao, X. Wu, Chem. Eng. J. 257 (2014) 36–44.
[37] Y.F. Rao, L. Qu, H. Yang, W. Chu, J. Hazard. Mater. 268 (2014) 23–32.
[38] Z. Sun, C. Liu, Z. Cao, W. Chen, Ultrason. Sonochem. 44 (2018) 86–96.
[39] T. Zhang, Y. Yang, X. Li, Y. Jiang, X. Fan, P. Du, H. Li, N. Wang, Z. Zhou, Environ. Technol. 42 (2021) 571–583.
[40] X. Xue, K. Hanna, C. Despas, F. Wu, N. Deng, J. Mol. Catal. A Chem. 311 (2009) 29–35.
[41] L. Mathurasa, S. Damrongsiri, Int. J. Recycl. Org. Waste Agric. 7 (2018) 143–151.
[42] J. Cao, S.B. Liaw, Y. Long, Y. Yu, H. Wu, Proc. Combust. Inst. 38 (2021) 4301–4308.
[43] M. Fan, C. Li, Y. Sun, L. Zhang, S. Zhang, X. Hu, Sci. Total Environ. (2021), 149354.
[44] O.D. Nartey, B. Zhao, Adv. Mater. Sci. Eng. 2014 (2014), 715398.